ADVANCED FUNCTIONAL MATERIALS

DOI: 10.1002/adfm.200600586

Supramolecular Nanostructuring of Silver Surfaces via Self-Assembly of [60]Fullerene and Porphyrin Modules**

By *Davide Bonifazi*,* *Andreas Kiebele*, *Meike Stöhr*, *Fuyong Cheng*, *Thomas Jung*,* *François Diederich*,* and *Hannes Spillmann**

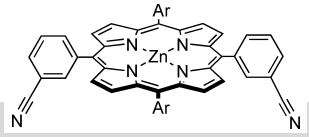

Recent achievements in our laboratory toward the "bottom-up" fabrication of addressable multicomponent molecular entities obtained by self-assembly of C_{60} and porphyrins on Ag(100) and Ag(111) surfaces are described. Scanning tunneling microscopy (STM) studies on ad-layers constituting monomeric and triply linked porphyrin modules showed that the molecules self-organize into ordered supramolecular assemblies, the ordering of which is controlled by the porphyrin chemical structure, the metal substrate, and the surface coverage. Specifically, the successful preparation of unprecedented two-dimensional porphyrin-based assemblies featuring regular pores on Ag(111) surfaces has been achieved. Subsequent co-deposition of C_{60} molecules on top of the porphyrin monolayers results in selective self-organization into ordered molecular hybrid bilayers, the organization of which is driven by both fullerene coverage and porphyrin structure. In all-ordered fullerene–porphyrin assemblies, the C_{60} guests organize, unusually, into long chains and/or two-dimensional arrays. Furthermore, sublimation of C_{60} on top of the porous porphyrin network reveals the selective long-range inclusion of the fullerene guests within the hosting cavities. The observed mode of the C_{60} self-assembly originates from a delicate equilibrium between substrate–molecule and molecule–molecule interactions involving charge-transfer processes and conformational reorganizations as a consequence of the structural adaptation of the fullerene–porphyrin bilayer.

1. Introduction

Organic nanomaterials hold exceptional promise to bring forth ultimate solutions in electronics, opto-electronics, photonics, energy storage, and medicine.[1–5] One of the major challenges that researchers in the field of nanomaterials face is that matter on the molecular scale can no longer be considered as a bulk entity. Rather, the role of both interface and surface become non-negligible and thus the properties of the materials are substantially affected, if not determined, by surface characteristics.[6] Scientists pursue two main approaches toward nanoscopic materials, known as "top-down" and "bottom-up".[5,7–10] Whereas established technologies in the "bottom-up" approach, i.e., the preparation of macroscopic materials based on the controlled assembly of molecular modules interconnected mainly by noncovalent bonding, are not yet available, this approach potentially offers significant advantages over any other methodologies for the controlled construction of large assemblies at the molecular level. Specifically, it enables simultaneous assembly of predetermined molecular modules and rapid for-

[*] Dr. D. Bonifazi
Dipartimento di Scienze Farmaceutiche, Università degli Studi di Trieste, Piazzale Europa 1, 34127 Trieste (Italy)
E-mail: dbonifazi@units.it
Dr. T. A. Jung
Laboratory for Micro- and Nanotechnology
Paul Scherrer Institute, 5232 Villigen PSI (Switzerland)
E-mail: thomas.jung@psi.ch
Prof. F. Diederich, Dr. F. Cheng
Laboratorium für Organische Chemie
ETH-Hönggerberg, HCI, 8093 Zürich (Switzerland)
E-mail: diederich@org.chem.ethz.ch
Dr. H. Spillmann, A. Kiebele, Dr. M. Stöhr
NCCR Nanoscale Science
Department of Physics, University of Basel,
Klingelbergstrasse 82, 4056 Basel, (Switzerland)
E-mail: h.spillmann@unibas.ch

[**] We gratefully acknowledge financial support by the Swiss National Science Foundation, the NCCR "Nanoscience", the Swiss Federal Commission for Technology and Innovation (KTI), and the European Union through the Marie-Curie Research Training Network PRAIRIES, contract MRTN-CT-2006-035810. We also thank Nanonis Inc. for the fruitful collaboration on the data acquisition system.

Davide Bonifazi was born in Guastalla (Italy) in 1975. After obtaining the "Laurea" from the University of Parma (1994–1999), and working with Prof. Enrico Dalcanale, he joined the group of Prof. François Diederich at the Swiss Federal Institute of Technology, Zürich (2000–2004). He was awarded the Silver Medallion of the ETH for his doctoral dissertation (2005). After a postdoctoral fellowship with Prof. Maurizio Prato at University of Trieste (2004–2005), he joined the Department of Pharmaceutical Science at the University of Trieste as research associate. Since September 2006, he has been at the Department of Chemistry at the "Facultés Universitaires Notre-Dame de la Paix" in Namur, Belgium, as a junior professor. His research interests focus on the self-assembly of electronically and optically active molecules, porphyrin chemistry, and functionalization of carbon nanostructures.

After an international childhood, Thomas Jung earned his Diploma degree in solid-state physics and biophysics from the ETH Zürich in 1987, working in the surface physics group of Prof. H.C. Siegmann. He joined the group of Prof. H.-J. Güntherodt to develop new experimental modes of the then emerging scanning probe microscopies to obtain his Ph.D. at the University of Basel in 1992. As a postdoctoral researcher he first joined the group of Prof. Ph. Avouris at the IBM TJ Watson research center. While he was working with Dr. J. K. Gimzewski at the IBM Zurich Research Laboratory, molecular positioning was achieved for the first time at room temperature and unique methods for the identification and analysis of an individual molecules' conformation were demonstrated. Thomas Jung's research contributions are highly cited in different scientific fields and have led to numerous invitations, e.g., as a visiting Professor at the University of Kyoto and the University of Madison Wisconsin. As a group leader in 'Molecular Nanoscience' both at PSI and at the University of Basel, Thomas Jung's research interest is focused on exploring new concepts for supramolecular assembly at surfaces and at addressing molecular bistabilities.

Born in the Grand Duchy of Luxemburg (1952), François Diederich studied chemistry at the University of Heidelberg (1971–1977). He joined the group of Prof. Heinz A. Staab for his diploma and doctoral theses, which he completed in 1979 with the synthesis of kekulene. Following postdoctoral studies with Prof. Orville L. Chapman at UCLA (1979–1981), investigating arynes in Argon matrices, he returned to Heidelberg for his Habilitation at the Max-Planck-Institut für Medizinische Forschung (1981–1985). Subsequently, he joined the faculty in the Department of Chemistry and Biochemistry at UCLA where he became a Full Professor of Organic and Bio-organic Chemistry in 1989. In 1992, he returned to Europe, joining the Department of Chemistry and Applied Biosciences at the ETH Zürich. His research interests, documented in more than 500 publications, are in the field of supramolecular chemistry, spanning dendritic mimics of globular proteins, molecular-recognition studies including structure-based drug design, and fullerene and acetylenic networks.

Hannes Spillmann was born in Zürich (Switzerland) in 1973. He graduated in Physical Chemistry in 1999 and obtained his doctorate in 2002 under the supervision of Prof. J. R. Huber and Prof. P. R. Willmott from the University of Zürich (Switzerland) with a thesis related to laser ablation and thin-film growth of ultrahard materials. He then joined the group of Prof. K. Kern at the Max-Planck-Institute for solid-state research in Stuttgart (Germany) as a postdoctoral researcher working on the self-assembly of metal–organic nanostructures and scanning tunnelling microscopy. In 2003, he became a scientific co-worker in the group of Prof. H.-J. Güntherodt at the University of Basel (Switzerland) and the Swiss National Center for Competence in Research (NCCR) in Nanoscale Science. His present work is focused on surface-supported bimolecular self-assembly with porphyrins and fullerenes.

mation of target structures under equilibrium conditions, which ensures self-correction of defects and long-range order.[7,8]

So far, noncovalent bonding has been mainly exploited both in solution and in the solid state to prepare extended periodic functional assemblies.[7–8,10–14] On the other hand, such molecular architectures formed in solution or in a crystal cannot be spatially addressed at the single-molecule level. Therefore, the most popular engineering approach employed in nanotechnology to probe local molecular properties and functions consists of the deposition of defined molecular modules on the surfaces of bulk materials such as metals, semiconductors, and insulators. Consequently, a large variety of examples of regular one- and two-dimensional assemblies, supramolecularly organized on surfaces through hydrogen-bonding,[15–17] dipole–dipole,[18] donor–acceptor,[19–21] van der Waals (vdW),[22,23] or even coordinative interactions[24–27] have recently been reported. Within these networks, functional molecular units are arranged into periodically ordered assemblies, thereby serving as potential templates for the engineering of single-molecule devices.

Chromophoric molecules, such as fullerenes[28,29] and porphyrins[30] with tunable highest occupied molecular orbital–lowest unoccupied molecular orbital (HOMO–LUMO) gaps and excited-state energies,[31,32] are appealing π-conjugated modules for the construction of functional molecular materials possessing exceptional electrochemical and photophysical properties. One of the most interesting aspects of C_{60} and porphyrins is that they spontaneously attract each other mainly through dispersion and donor–acceptor interactions,[27] as experimentally determined both in solution[33] and in the solid state.[34] Following the first reports on a fullerene-containing donor–acceptor dyad,[19] a large number of supramolecular and covalent fullerene–porphyrin conjugates have been prepared and studied for their conformational, electrochemical, and photophysical properties.[35–41]

We decided to take advantage of the fullerene–porphyrin affinities to selectively engineer supramolecular assemblies on surfaces with a large periodicity. Characterizing these assemblies by scanning probe methods, such as scanning tunneling microscopy (STM),[42] provides a detailed insight into the structures at the molecular and atomic levels. A limited number of studies has been undertaken to elucidate the supramolecular behavior of single porphyrin molecules on surfaces.[43–46] In particular, their assembly with other redox- and/or photoactive molecular species, such as fullerenes, on surfaces has not been fully investigated.[47,48] Herein, we describe the advances made in our laboratory towards the "bottom-up" fabrication of organic nanopatterned surfaces based on 2D supramolecular assemblies composed of porphyrins and C_{60} on Ag(100) and Ag(111). Two types of porphyrin macrocycles were considered in this investigation (for details on parts of this work, see communications by Diederich and co-workers[49,50]): bis(3-cyanophenyl)-substituted monomer **1** and a series of triply fused diporphyrins (**2**–**4**) (Fig. 1). We show that the patterning of these surfaces is controlled by the chemical structure of the porphyrin, the metal substrate, and the surface coverage. In particular, we report the preparation of 2D porphyrin-based supramolecular porous network structures on Ag(111) at low surface coverage, which are capable of complexing C_{60} molecules in a periodic array of hosting cavities. In addition, fullerene mobility within the porphyrin networks and repositioning experiments conducted with the STM tip are described. Contemporaneous with our investigations, the groups of Itaya and Komatsu have also reported the preparation of hybrid bicomponent monomolecular layers constituted of [60]fullerene derivatives self-assembled on top of a pre-organized Zn^{II}-octaethylporphyrin [Zn(OEP)] monolayer on Au(111) surfaces.[51] Specifically, supramolecular 1:1 [60]fullerene/[Zn(OEP)] complexes in which an open-cage [60]fullerene derivative is centrally nested atop the tetrapyrrolic core have been observed, showing that the molecular orientation of the fullerene ad-layers was fully controlled by the underlying [Zn(OEP)] monolayer.[51]

2. Binary Molecular Layers of Monomeric Porphyrin 1 and C_{60}

2.1. Deposition and Self-Assembly of Porphyrin 1 on Ag(100) and Ag(111) Surfaces

The first step in the formation of self-assembled patterned surfaces is the deposition of porphyrin macrocycle **1** onto clean

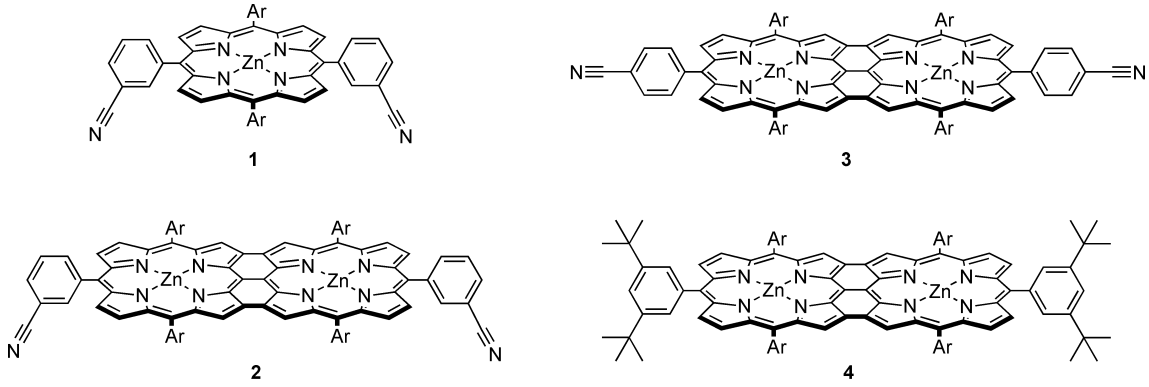

Figure 1. Chemical structure of the porphyrin derivatives used in this investigation.

Ag(100) and Ag(111) surfaces under ultrahigh-vacuum (UHV) conditions. High-resolution STM images taken on an Ag(100) substrate at full surface coverage, ca. 1.0 ML (ML = monolayer), revealed that the porphyrin molecules arrange themselves into rows along the <110> direction of the underlying Ag(100) substrate, leading to the **1** → Ag(100) assembly outlined in Figure 2a (see also proposed network model on the right).[49] In accordance with earlier experiments conducted on tetra-substituted porphyrin derivatives bearing four 3,5-di(*tert*-butyl)phenyl moieties in the meso positions, the preferential tunneling current transport for these molecules occurs through these substituents.[52,53] Since the 3-cyanophenyl residues and the central porphyrin core do not contribute to the tunneling current on such silver surfaces, each single porphyrin molecule is imaged as a group of two bright aligned lobes separated by ca. 1.2 nm (see Fig. 2a, left). The latter value is in good agreement with the intramolecular distance between the two 3,5-di(*tert*-butyl)phenyl substituents (center-to-center distance: 1.26 nm), as measured from the crystal structure of **1**.[33,49] In accordance with the previous reports, our high-resolution STM data (Fig. 2a) are also consistent with porphyrin molecules lying flat on the metal substrate and not overlapping with their neighbors. Notably, all lobes appear with the same apparent height, suggesting that the interplanar angle between the 3,5-di(*tert*-butyl)phenyl moieties and the porphyrin plane is equal for all molecules embedded within the entire monolayer. At low surface coverage, 0.2–0.5 ML, a 2D gas phase was observed in dynamic equilibrium with ordered porphyrin islands. No reorganization of the **1** → Ag(100) assembly was observed upon thermal annealing at 450 K.

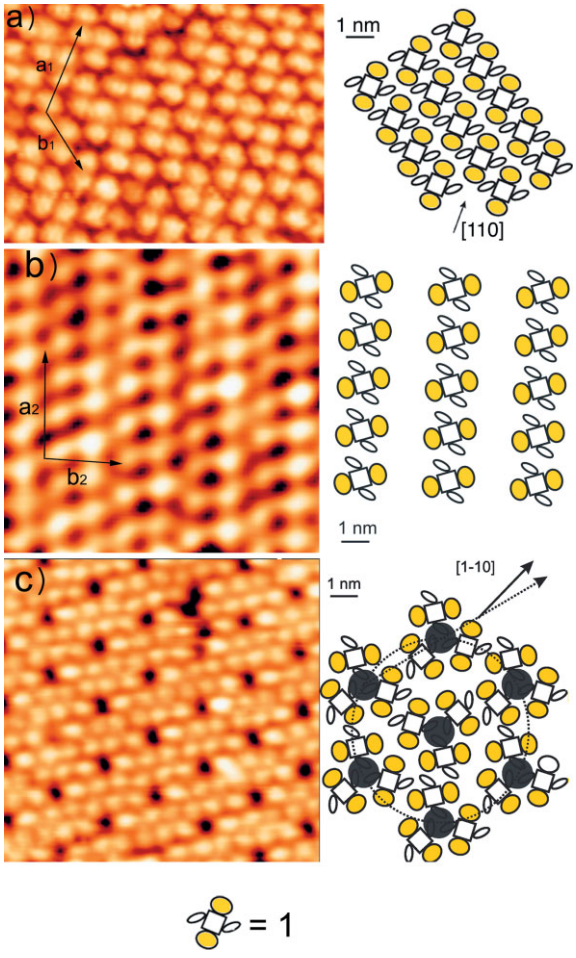

Figure 2. a) Left: detailed STM image (scan range: 12.2 nm × 9.1 nm, V_{bias} = 2.80 V, I_t = 72 pA, T = 298 K) of a full-coverage monolayer of porphyrin **1** sublimed on Ag(100); the distance between the centers of two neighboring molecular subunits is (2.4 ± 0.1) nm along the a_1 direction and (1.5 ± 0.1) nm along the b_1 direction; the molecular rows along directions a_1 and b_1 cross each other at an angle of 126° ± 5°. Right: Proposed surface pattern of the self-assembled monolayer on Ag(100). Reproduced with permission from [49]. b) Left: detailed STM image (scan range: 14.0 nm × 13.5 nm, V_{bias} = 2.78 V, I_t = 18 pA, T = 298 K) of a full-coverage monolayer of porphyrin **1** sublimed on Ag(111) after annealing at 450 K. The distance between the centers of two neighboring molecular subunits is (1.8 ± 0.1) nm along the a_2 direction and (3.3 ± 0.1) nm along the b_2 direction; the molecular rows along directions a_2 and b_2 cross each other at an angle of 92° ± 4°. c) Left: detailed STM image (scan range: 17.7 nm × 16.9 nm, V_{bias} = 2.96 V, I_t = 25 pA, T = 298 K) of less than a monolayer of porphyrin **1** sublimed on Ag(111), showing the presence of a porous monolayer. Each porphyrin molecule appears as two bright protrusions, which are separated by ca. 1.2 nm. Right: Proposed model of the self-assembled porous network ($\alpha \approx 15°$).

Porphyrin **1** was also sublimed on Ag(111) under the same coverage conditions (ca. 1 ML). While at 298 K the molecules do not form an ordered phase; after annealing at 450 K, the porphyrin modules assemble into supramolecular **1** → Ag(111) rows, shown in Figure 2b (left). The intraporphyrin distances along the a_2 and b_2 directions are (1.8 ± 0.1) nm and (3.3 ± 0.1) nm, respectively. Again, each molecule is represented as a group of two lobes that correspond to the 3,5-di(*tert*-butyl)phenyl moieties (Fig. 2b, left). In contrast to the case of Ag(100), the lobes do not appear with the same apparent height. Although full rotation of the 3,5-di(*tert*-butyl)-phenyl substituents about the phenyl–porphyrin σ-bonds is partially hindered by the C–H bonds at the β-positions, they have a certain degree of freedom to rotate.[53] Therefore, the reason for the protrusions appearing with distinct heights is attributable to different conformations adopted by the 3,5-di(*tert*-butyl)phenyl moieties within the monolayer.[53]

At low surface coverage, ca. 0.5–0.7 ML, porphyrin macrocycle **1** exceptionally organizes in a porous (p) assembly (p**1** → Ag(111), Fig. 2c, left). A structural model of the porphyrin ad-layer is also shown in Figure 2c (right).[50] The highly organized hexagonal superstructure is constituted of discrete pores and is rotated by 15 ± 4° with respect to the [1–10] direction of the underlying Ag(111) substrate, showing a periodicity of (3.3 ± 0.1) nm. The assembly was also revealed to be thermally stable upon annealing at up to 448 K. In the proposed model (Fig. 2c, right), the 3-cyanophenyl residues are arranged in trimeric units surrounding a central cavity. The cross section taken from the STM images of p**1** → Ag(111), shown in Figure 3, characterizes the typical pore geometry with a diameter and a depth of approximately 1.2 and 0.12 nm, respectively. Owing to the finite size of the STM tip, the cavity dimensions are affected by the tip–surface convolution, which reduces the real dimensions of the pore. In the low-density molecular regions, such as in proximity to the step edges of the Ag(111) surface, a 2D gas phase in equilibrium with the ordered p**1** → Ag(111) assem-

ADVANCED FUNCTIONAL MATERIALS

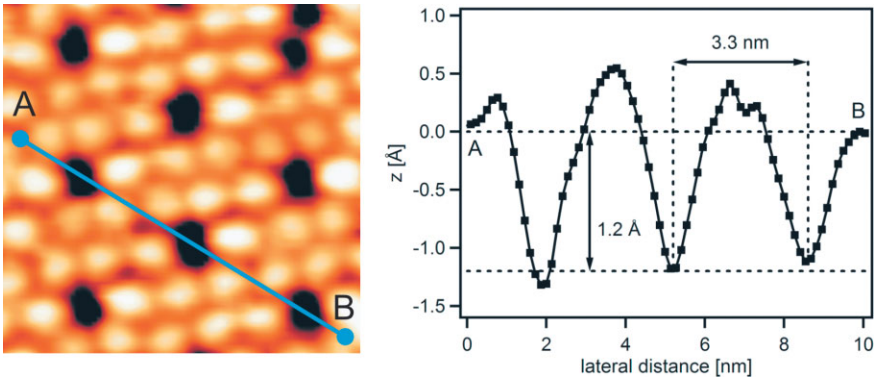

Figure 3. Left: detailed STM image (scan range: 9.1 nm × 8.9 nm, $V_{bias} = 2.96$ V, $I_t = 25$ pA, $T = 298$ K) of the porous **1**-based network on Ag(111). Right: Cross-section profile of three consecutive pores (from A to B).

bly is also localized, as is evidenced from molecular fluctuations at the borders of the condensed porous network in time-lapsed imaging sequences. The latter observation confirms the presence of small diffusion barriers for porphyrin **1** on Ag(111), as observed for the assemblies on Ag(100).

2.2. Hosting Properties of the 1-Based Ad-Layers

In order to investigate the hosting properties of the porphyrin networks described above, C_{60} molecules were sublimed on top of the preformed porphyrin assemblies. Sublimation of approximately 0.02 ML of C_{60} on top of a full monolayer of **1** on Ag(100) resulted in the predominant formation of randomly distributed single molecules and clusters of fullerene on top of the porphyrin assembly (Fig. 4a). Interestingly, all the single fullerene units were revealed to be static, accounting for a high-energy mobility barrier probably caused by the strong fullerene–porphyrin chromophoric interaction and the friction effect originating from the 3,5-di(*tert*-butyl)phenyl groups. Such tangled hybrid bilayers were stable over a wide range of temperatures, and after annealing at 450 K, no further evolution of the fullerene organization was evidenced.

Deposition of ca. 0.14 ML of C_{60} onto ca. 0.85 ML of **1** preadsorbed on Ag(111) (i.e., the **1** → Ag(111) assembly) resulted in the segregation of two molecular domains: i) $2\sqrt{3} \times 2\sqrt{3}\,R30°$ islands of C_{60} (where R represents the rotational angle between the crystallographic direction of the hexagonal C_{60} monolayer and that of the hexagonal Ag(111) surface), and ii) a condensed **1** → Ag(111) network. However, thermal annealing (450 K) of the segregated layers resulted in an unprecedented C_{60}–porphyrin assembly ((C_{60}-**1**) → Ag(111)), shown in Figure 4b. The porphyrin ad-layer shows a completely different molecular packing if compared to the molecular arrangement adopted in the **1** → Ag(111) assembly (Fig. 2). The carbon spheres are arranged in vertically aligned pairs (i.e., supramolecular fullerene "dumbbells", intrapair $C_{60}\cdots C_{60}$ distance of 2.3 nm). This "dumbbell" pattern is repeated approximately every 7.5 and 6.0 nm in the horizontal and vertical directions, respectively, and results in exceptionally large domains (up to 50 nm × 100 nm). Notably, missing fullerenes reveal that the underlying porphyrin layer features a completely close-packed structure (see lower right corner in Fig. 4b), strongly supporting the assumption that, in the (C_{60}-**1**) → Ag(111) assembly, the C_{60} molecules are located on top of the porphyrin layer, detached from the underlying Ag(111) substrate.[50] Regrettably, we could not precisely estimate the location of the C_{60} molecules with respect to the underlying monolayer of **1** within the (C_{60}-**1**) → Ag(111) assembly. Nevertheless, the high thermal stability and the absence of fullerene mobility account for a high-energy corrugation and strong interaction within the hybrid assembly that we here tentatively ascribe to the favorable fullerene–porphyrin interaction[27] (interaction energy 16–18 kcal mol^{-1} (1 kcal = 4.186 kJ) as calculated for monomeric porphyrins). Moreover, the latter observation suggests that the monolayer corrugation and the fullerene–porphyrin chromophoric interaction are together stronger than the thermal energy at 298 K (i.e., ≫ 2.48 kJ mol^{-1} or 0.59 kcal mol^{-1}). These observations on the (C_{60}-**1**) → Ag(111) assembly are in agreement with our recent results obtained in solution, where fullerene–porphyrin conjugates show a strong interchromophoric interaction as evidenced by transient UV-vis absorption and ^{1}H NMR spectroscopies.[33,54]

Sublimation of C_{60} on top of the p**1** → Ag(111) assembly resulted in the confinement of the C_{60} molecules in the pore sites (Fig. 4c, left). No C_{60} molecules were found to adsorb on top of individual porphyrin units, as observed for the porphyrin–fullerene assembly (C_{60}-**1**) → Ag(111) outlined in Figure 4b. Time-lapsed STM images revealed a considerable lateral mobility of the C_{60} guests within the porphyrin assembly.[55] The C_{60} guests hop from pore to pore at a rate of ca. 10^{-3} s^{-1} in the low-coverage regime (0.01 ML C_{60}) at 298 K. A comprehensive study of the mobility mechanisms of fullerene guests as a function of the fullerene structure (C_{60} and C_{70}) and the coverage in 2D nanoporous networks on Ag(111) has been reported elsewhere.[56] Increasing the coverage of adsorbed C_{60}, from 0.01 to 0.02 ML, results in condensation of the guest molecules into large fullerene islands. Besides single C_{60} molecules, linear hosted fullerene chains constituting several fullerene units have also been observed. Notably, all the (C_{60}-**1**) → Ag(111) fullerene-based patterns exhibit dynamical changes, e.g., by assembling and disassembling of the observed chains and islands, as time proceeds.[50] A further increase of the fullerene coverage to about 0.07 ML (Fig. 4d, left), leads to a change of the short, scattered fullerene chains into branched lines and large islands.[50] At a high fullerene coverage, ca. 0.1 ML (Fig. 4e, right), almost all pores were found to be occupied by a C_{60} molecule and the mobility of the guest molecules within the porphyrinic network was drastically reduced.[50] Further increase of the C_{60} coverage (> 0.1 ML) causes the irreversible collapse of the regular fullerene–porphyrin (C_{60}-p**1**) → Ag(111) assembly, leading to the formation of a disordered intermixed phase at 298 K. Interestingly, the thermal annealing

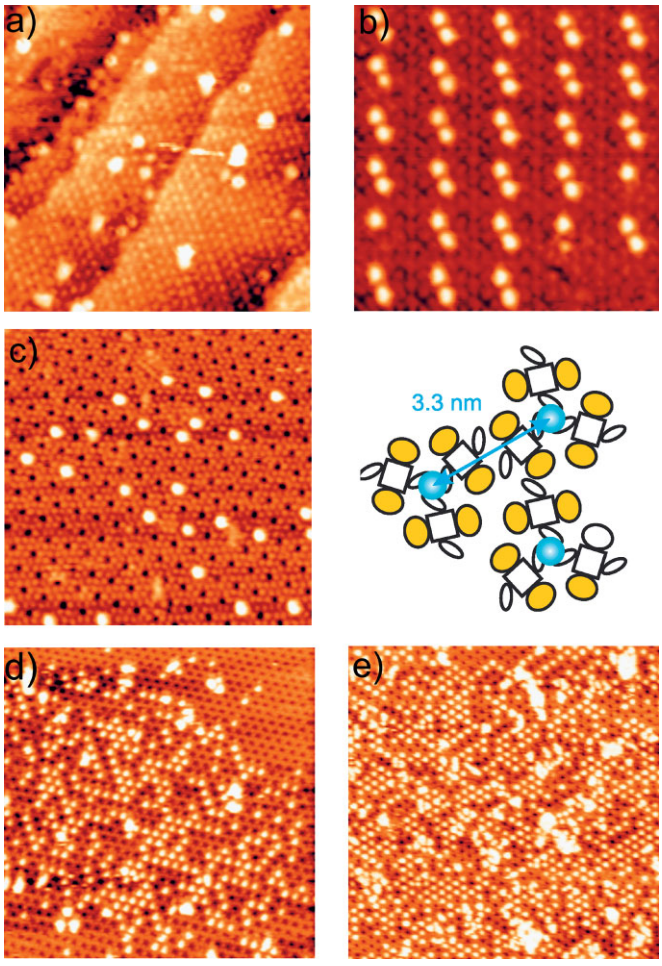

Figure 4. a) STM images (scan range: 50 nm × 50 nm, V_{bias} = 3.01 V, I_t = 10 pA, T = 298 K) of the C_{60}-**1** assembly on Ag(100) revealing the presence of fullerene aggregates and disordered individual C_{60} molecules. b) Supramolecular assembly of C_{60}-**1** obtained after annealing (453 K) of ca. 0.14 ML of C_{60} and a preadsorbed ca. 0.85 ML of **1** on a Ag(111) substrate (scan range: 33 nm × 33 nm, I_t = 12 pA, V_{bias} = 2.63 V). c) Left: STM image of the hybrid C_{60}-**1** assembly on Ag(111) (0.01 ML of C_{60}, scan range: 49.8 nm × 48.0 nm, V_{bias} = 2.85 V, I_t = 9 pA, T = 298 K). Right: proposed model for the C_{60}-**1** assembly on Ag(111). The fullerene molecules (blue spheres) are located in the center of the pores approximately on top of the 3-cyanophenyl residues. d-e) STM images of the (C_{60}-p**1**) → Ag(111) assembly after deposition of 0.07 ML (left, scan range: 100 nm × 100 nm, V_{bias} = 3.0 V, I_t = 9 pA, T = 298 K) and 0.1 ML (right, scan range: 111 nm × 112 nm, V_{bias} = 3.0 V, I_t = 12 pA, T = 298 K) of C_{60} revealing a nonstochastic distribution of the fullerene guests which are temporarily condensed into chain- and islandlike assemblies. Reproduced with permission from [50].

of the latter disordered hybrid phase (C_{60} deposition > 0.1 ML) at 450 K resulted in partial formation of the stable and ordered fullerene–porphyrin bilayers ((C_{60}-**1**) → Ag(111)) shown in Figure 4b, while the annealing of any hybrid (C_{60}-p**1**) → Ag(111) assemblies in the low-coverage fullerene regime (between 0.01 and 0.1 ML) led to phase separation into pure porous porphyrin domains and $2\sqrt{3} \times 2\sqrt{3}\,R30°$ fullerene islands. The latter evidence supports our assumption about the weak physisorptive nature of the interactions existing in the hybrid fullerene–porphyrin (C_{60}-p**1**) → Ag(111) assembly.

As support for this temperature-dependent rearrangement, a detailed STM image of the assemblies after thermal annealing of a hybrid ad-layer containing ca. 0.2 ML of C_{60} deposited onto ca. 0.89 ML of **1** pre-adsorbed on Ag(111) is displayed in Figure 5. One can clearly distinguish the co-existence of the two different fullerene–porphyrin assemblies: the fullerene hosted in the pores (lower left corner,

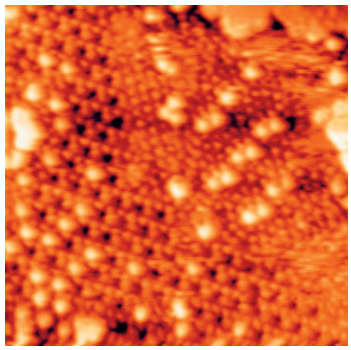

Figure 5. Detailed STM image of the two ordered "porous" and "dumbbell" phases co-existing after thermal annealing at ca. 450 K of a hybrid system constituted of ca. 0.2 ML of C_{60} sublimed onto a preadsorbed ca. 0.9 ML of **1** on Ag(111) (scan range: 50 nm × 50 nm, I_t = 11 pA, V_{bias} = 2.83 V, T = 298 K).

(C_{60}-p**1**) → Ag(111)) and the paired arrangement (upper right corner, (C_{60}-**1**) → Ag(111)). Moreover, the different porphyrin networking in the porous p**1** → Ag(111) phase is easily discernible from that of the "rearranged" porphyrin phase underlying the supramolecular dumbbell (C_{60}-**1**) → Ag(111) assembly (Fig. 5, center and upper right part).

A schematic diagram summarizing the temperature- and coverage-dependent formation of the different **1**-based assemblies on Ag(111), with and without C_{60}, is shown in Figure 6.

3. Binary Layers of C_{60} and Triply Linked Diporphyrins

3.1. Deposition and Self-Assembly of Triply Fused Diporphyrins 2–4 on Ag(100) and Ag(111) Surfaces

High-resolution STM images taken on a Ag(100) substrate covered with a 0.2–0.5 ML of diporphyrin **2** showed the coexistence of two phases: 2D ordered islands in dynamic equilibrium with a 2D gas phase.[49] Evidence for this 2D molecular gas phase was obtained from the fluctuation of the borders of the condensed islands in time-lapsed imaging sequences. In the STM images (Fig. 7a), individual molecules are represented as groups of four lobes arranged in a slightly distorted square shape. In analogy to previous studies on similarly substituted porphyrins,[53] we assume that the diporphyrin macrocycle is lying flat on the silver surface, as in the case of monomer **1**. Each lobe in the STM image results again from preferential tunneling transport through the 3,5-di(*tert*-butyl)phenyl substituents.[53] The observed size of the four-lobed shape is about

ADVANCED FUNCTIONAL MATERIALS

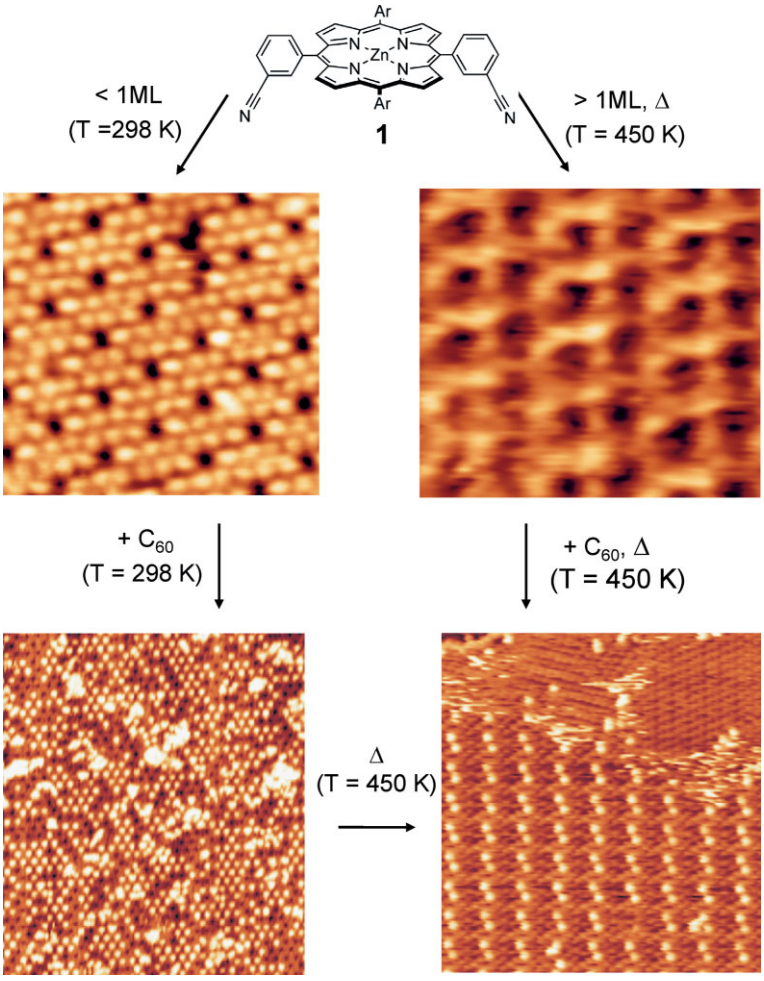

Figure 6. Schematic diagram of the surface- and temperature-dependent polymorphed C_{60}-**1** assemblies on Ag(111).

0.9 nm × 0.7 nm, which is consistent with the molecular dimensions of **2** as estimated by PM3-based geometry optimization and seen in the crystal structure of a similar compound reported by Osuka and co-workers.[57,58] As described for the case of porphyrin monomer **1**, the different apparent heights of the protrusions in the STM image reflect the different conformations of the 3,5-di(*tert*-butyl)phenyl substituents partially rotating around the phenyl–porphyrin σ-bonds. Moreover, consecutive time-lapsed images reveal the presence of a certain conformational dynamicity of the porphyrin system: reversible changes manifest themselves in the alternating (blinking) "dim" and "bright" appearance of the 3,5-di(*tert*-butyl)phenyl substituents. These observations are further discussed in Section 2.3 below.

Under the same conditions, porphyrin dimer **2** was sublimed on Ag(111) (Fig. 7b). In agreement with the **2** → Ag(100) assembly, the molecules appear as four lobes arranged in a squarelike shape. The closest distances between the lobes are approximately 1.2 and 0.8 nm along the b_4 and a_4 directions, respectively, as shown in Figure 7b, which are consistent with the molecular dimensions as measured on Ag(100). Diporphyrin **2** self-organizes into regular molecular rows that are clearly discernible in the STM images (see the molecular model shown in Fig. 7b, right).[49]

In order to unravel the role of the C≡N residues, the two triply fused diporphyrins **3** and **4**, bearing two 4-cyanophenyl and 3,5-di(*tert*-butyl)phenyl substituents, respectively, were investigated as reference compounds (Fig. 1). At high porphyrin coverage (ca 1.0 ML), diporphyrin **3** self-organizes into regular molecular rows clearly distinguishable in the STM images (Fig. 8a, left). Contrary to the square-shaped appearance of diporphyrin **2** in the STM images, molecule **3** comes into view as a group of four lobes arranged in a rhombic figure. We attribute this appearance to a change in conformation adopted by the four 3,5-di(*tert*-butyl)phenyl substituents. In accordance with this interpretation, the phenyl moieties attached to the fused diporphyrin cores are tilted, such that a rhombic disposition of the lobes results ("crossed legs" conformation, Fig. 8b right).[59] We estimated from pure geometrical considerations that the rotation angle around the σ-bond connecting the phenyl substituent and the porphyrin scaffold is ca. 30° (ϕ angle in Fig. 8b, left). This model is consistent with the conformational assignment of "lander" molecules deposited onto Cu(001), obtained from STM data by Berndt and co-workers.[59] Moreover, in accordance with the intermolecular distances measured in the STM images, and thus with the proposed model (Fig. 8a, right), the phenyl substituents also need to be distorted by around 30° with respect to the axis normal to the silver surface (angle φ in Fig. 8b, left). Such types of strong molecular deformations have been described by Moresco et al. for similar porphyrins.[60,61] The reason for such a distorted molecular conformation can be tentatively ascribed to two factors: i) the 4-cyanophenyl substituents are most probably lying parallel to the silver surface, thus allowing further bending or twisting of the 3,5-di(*tert*-butyl)phenyl moieties compared to the 3-cyanophenyl derivative **2**; ii) a very short intermolecular distance along the a_5 direction, compared to those measured for the **2** → Ag(100) and **2** → Ag(111) assemblies, have been observed (see caption to Fig. 8), as manifested by the high density of the **3** → Ag(111) assembly.

Contrary to all C≡N-bearing porphyrinoids investigated in this work, compound **4**, lacking cyano groups, does not form any appreciable ordered network at comparable monolayer coverage, on either Ag(111) and Ag(100) (Fig. 9). STM images of the disordered **4** → Ag(100) network show spiking areas that are in continuous evolution, revealing the presence of mobile molecules over the whole ad-layer. The observed dynamicity of such an assembly accounts for the presence of intermolecular and molecule–substrate interactions that are weaker than the thermal energy at 298 K.

From the observations obtained with the nonordered assembly of **4**, the presence of strong dipolar residues, such as the C≡N groups in diporphyrins **2** and **3**, seems to be crucial for

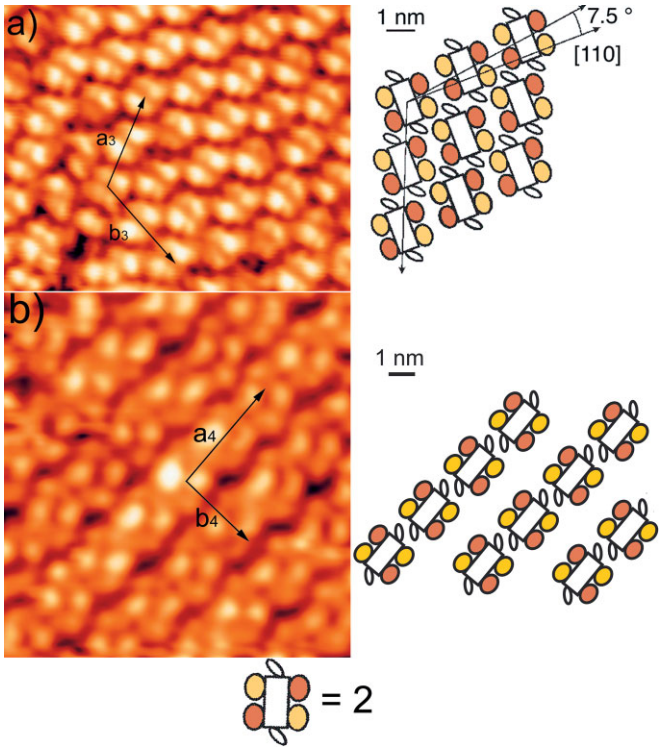

Figure 7. a) Left: STM image (scan range: 15.8 nm × 11.9 nm, V_{bias} = 2.5 V, I_t = 72 pA, T = 298 K) of a full-coverage monolayer of **2** sublimed on Ag(100); the distance between the centers of two neighboring molecules is (2.2 ± 0.1) nm along the a_3 direction and (2.3 ± 0.1) nm along the b_3 direction; the molecular rows cross each other at an angle of 120° ± 5° along the direction a_3 and b_3. Reproduced with permission from [49]. Right: proposed surface pattern of the self-assembled monolayer of diporphyrin **2** on Ag(100). Reproduced with permission from [49]. b) Left: STM image (scan range: 17 nm × 17 nm, V_{bias} = 2.62 V, I_t = 13 pA, T = 298 K) of a full-coverage monolayer of diporphyrin **2** sublimed on Ag(111). The distance between two centers of each molecular subunits is (2.1 ± 0.1) nm along the a_4 direction and (2.7 ± 0.1) nm along the b_4 direction. The molecular rows along the direction a_4 and b_4 cross each other at an angle of 90° ± 3°. Right: proposed surface pattern of the self-assembled monolayer of diporphyrin **2** on Ag(111). The yellow and brown lobes reflect the heights attributed to the different conformation adopted by the 3,5-di(*tert*-butyl)phenyl legs as displayed by the dissimilar intensity tunneling current.

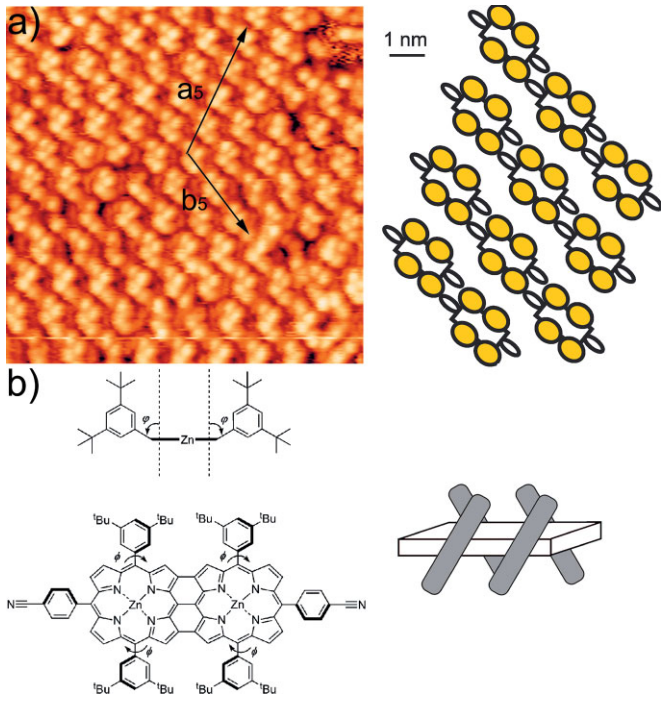

Figure 8. a) Left: STM image (scan range: 13.9 nm × 13.2 nm, V_{bias} = 2.86 V, I_t = 13 pA, T = 298 K) of a full-coverage monolayer of diporphyrin **3** sublimed on Ag(100). The distance between two centers of each molecular subunits is (1.9 ± 0.1) nm along the a_5 direction and (2.2 ± 0.1) nm along the b_5 direction. The molecular rows along the direction a_5 and b_5 cross each other at an angle of 120° ± 5°. Right: proposed surface pattern of the self-assembled monolayer of diporphyrin **3** on Ag(100). b) Schematic chemical structure of porphyrin **3** showing the conformational constrains in which the 3,5-di(*tert*-butyl)phenyl moieties are forced to adopt such that a rhombic disposition of the lobes results.

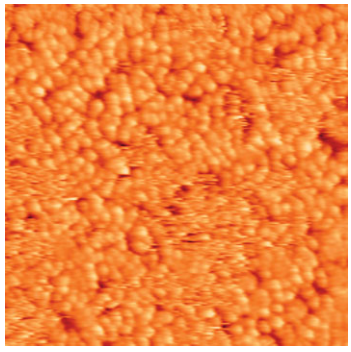

Figure 9. STM image (scan range: 30 nm × 30 nm, V_{bias} = 2.92 V, I_t = 20 pA, T = 298 K) of a full-coverage monolayer of hexakis(3,5-di(*tert*-butyl)phenyl)diporphyrin **4** sublimed on Ag(100). Only a disordered phase was observed as a consequence of the high mobility of the molecular units.

the formation of ordered porphyrin-based assemblies. Therefore, it can be deduced that the order and thermal stability of the C≡N-containing assemblies are likely to be strongly influenced and directed by dipolar interactions occurring between the C≡N residues of neighboring molecules.[18,62] This has also been observed in the crystal lattice of porphyrin monomer **1**, where C≡N residues interact pairwise via dipolar forces.[33] This intermolecular, dipolar stabilizing effect is enhanced by higher surface coverages, which force the molecules to closely pack and consequently to adopt a specific conformation. In the case of the assemblies containing molecules **1** and **2**, the 3-cyanophenyl moieties could, in principle, adopt two positions: one with the cyano group pointing toward the silver surface, and another with these groups oriented away from the surface. Further experimental and computational investigations will be required to clarify possible energetic contributions of the cyano groups to physisorption on the surfaces.

3.2. [60]Fullerene Ad-Layers Organized on 2–4 Assemblies

Sublimation of ca. 0.02 ML of C_{60} on top of a full monolayer of **2** on Ag(100) resulted in the predominant formation of unidirectional chains of various lengths composed of several bright protrusions (Fig. 10, left).

ADVANCED FUNCTIONAL MATERIALS

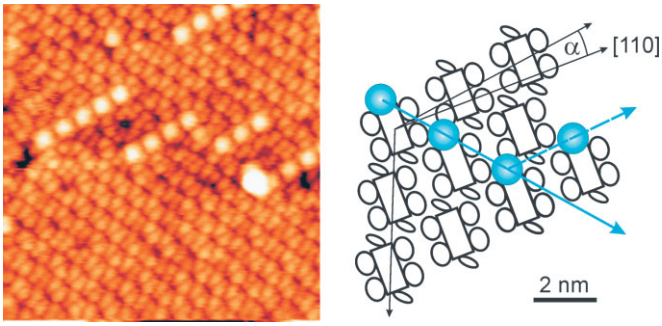

Figure 10. STM images of C_{60}-**2** assemblies on Ag(100). Left: STM image (scan range: 30 nm × 30 nm, $V_{bias} = 3.01$ V, $I_t = 12$ pA, $T = 298$ K) showing the favored direction of the chain-like assembly of C_{60} on a full-coverage monolayer of diporphyrin **2** sublimed on Ag(100). Right: proposed surface pattern of the C_{60}-**2** assembly; the fullerene molecules (blue spheres) are located between the porphyrin units. Reproduced with permission from [49].

No 2D islands composed of C_{60} have been detected. Each protrusion exhibits a height of (0.44 ± 0.02) nm measured with respect to the porphyrin layer. Owing to their spherical appearance in the STM data, the protrusions can be identified as single C_{60} molecules.[63] The longest chains (ca. 15.5 nm) are composed of eight C_{60} molecules with an intermolecular $C_{60}\cdots C_{60}$ distance of approximately 2.2 nm. The supramolecular structure of the bimolecular C_{60}–diporphyrin assembly $((C_{60}\text{-}\mathbf{2}) \rightarrow Ag(100))$ that best resembles the STM images is depicted in Figure 10 (right). Despite the large surface area of the fused macrocyclic core (about 1 nm^2), the adsorbed fullerene molecules are located away from the porphyrin plane and precisely assembled between three neighboring molecules on top of the 3-cyanophenyl substituents. This behavior is possibly promoted by the interaction between the electronegative N(cyano) atoms and the electropositive surface of the carbon sphere.[21] At 298 K, the C_{60} molecules do not diffuse within the assembly, indicating that the corrugation of the C_{60}–substrate interactions is stronger than the thermal energy. Notably, the $(C_{60}\text{-}\mathbf{2}) \rightarrow Ag(100)$ assembly disrupts at 423 K, leading to a phase separation into pure porphyrin domains and $2\sqrt{3} \times 2\sqrt{3}\,R30°$ hexagonal fullerene islands. In order to rule out the possibility that the C_{60} molecules are inserted in the porphyrin domains as a self-intermixed phase,[63] as in the case of subphthalocyanine and C_{60} assemblies, single-molecule-repositioning experiments of the carbon spheres were performed. After an STM relocation sequence, the former fullerene sites clearly remained unaffected and were occupied only by molecule **2,** proving that the C_{60} molecules sit on top of a dense monolayer.[49]

In order to better understand the intermolecular interaction between the fullerene guests and the diporphyrin ad-layers, we inverted the deposition order, subliming first C_{60} and then porphyrin molecule **2** (see Fig. 11) on top. Sublimation of C_{60} (0.5 ML) on a Ag(111) surface led to the formation of a partial monolayer organized into hexagonal $2\sqrt{3} \times 2\sqrt{3}\,R30°$ domains. Deposition of porphyrin **2** on top of the fullerene layer, held at 298 K, resulted in the formation of slightly disordered agglomerates of diporphyrin **2** on top of the ordered C_{60} layer, as

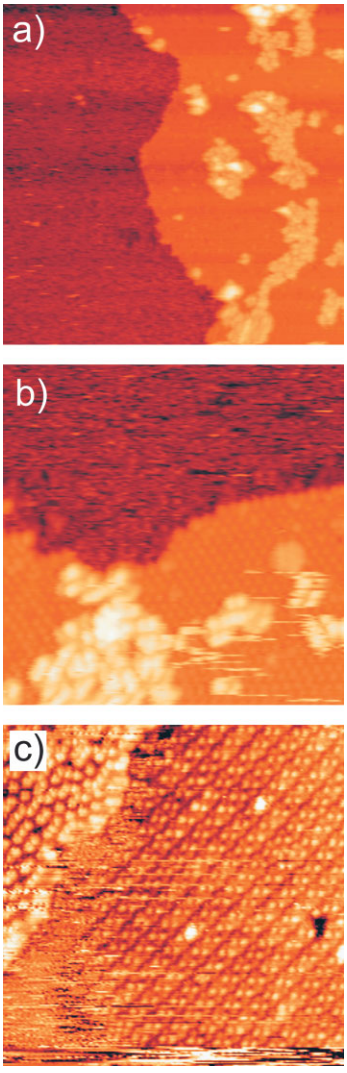

Figure 11. STM images of **2**-C_{60} assemblies on Ag(111). a) STM image (scan range: 100 nm × 100 nm, $V_{bias} = 2.1$ V, $I_t = 15$ pA, $T = 298$ K) showing the formation of disordered agglomerates of diporphyrin **2** upon adsorption of the porphyrin molecules (ca. 0.5 ML) on ordered C_{60} islands. b) Detailed view (scan range: 30 nm × 30 nm, $V_{bias} = 2.5$ V, $I_t = 15$ pA, $T = 298$ K): the porphyrin molecules at the border of the agglomerates show a limited mobility on the fullerene layer, accounting for the presence of a weak interaction between the two molecular species. In contrast, the spiky area in the upper part of the STM image is caused by highly mobile diporphyrin molecules diffusing on the bare Ag(111) substrate. c) STM image (scan range: 42.4 nm × 42.4 nm, $V_{bias} = 2.8$ V, $I_t = 12$ pA, $T = 298$ K) showing the phase separation between the fullerene and porphyrin molecules after thermal annealing to 450 K. Only a few scattered C_{60} molecules are found on the porphyrin monolayer.

shown in Figure 11a. The fuzzy imaging of the diporphyrins on top of the ordered fullerenes (see also Fig. 11b) strongly indicates that the diporphyrins at the border of such agglomerates are laterally displaced under the influence of the scanning STM tip.[64] From this observation, we thus extrapolated that the fullerene–diporphyrin interaction and the corrugation energy between the porphyrin guest and the hosting $C_{60} \rightarrow Ag(111)$ monolayer combined are lower than in the previously reported

reverse case, where C_{60} is located on top of diporphyrin **2** (see Fig. 10). This low affinity of the $C_{60} \rightarrow Ag(111)$ assembly towards porphyrin guests may possibly be explained by considering two effects: a) the charge-transfer process taking place from the Ag(111) substrate to the fullerene monolayer saturating the fullerene electron-accepting capabilities; and b) despite the great electron-donating properties, the **2**-centered, low-lying, and short-lived singlet-energy level[33,41] does not allow for the formation of any charge-separated state, namely any strong chromophoric interactions. Thermal annealing (at 450 K) of the (**2**-C_{60}) → Ag(100) assembly gives rise to a complete phase separation (Fig. 11c): disordered fullerene islands (left upper corner) and an ordered network of **2** (right down corner), assembled in the same manner as the one shown in Figure 7b, appear. Only a few scattered, fixed C_{60} molecules have been observed on top of the **2**-based domains.

4. Rationale

Apart from the (C_{60}-**1**) → Ag(100) assembly, in which a stochastic distribution of the fullerene ad-layer has been observed, all other fullerene–porphyrin assemblies show the presence of exceptionally ordered nanostructures. The formation of such regular hybrid networks could possibly be explained by considering the presence of net long-range attractive or cohesive intermolecular forces between the fullerene molecules. However, the large $C_{60}\cdots C_{60}$ distance measured in all ordered superstructures (the shortest $C_{60}\cdots C_{60}$ distance measured for the (C_{60}-**2**) → Ag(100) assembly is ca. 2.2 nm), excludes the presence of any effective $C_{60}\cdots C_{60}$ interaction (31 kcal mol^{-1} at a separation of 1 nm).[65] Additional evidence for a unique interplay between network constituents and the surface can also be deduced from the time-lapsed series of high-resolution images of porphyrins **1** and **2** on Ag(111). Fluctuating bright–dim patterns, which are attributed to rotations of the 3,5-di(*tert*-butyl)-phenyl substituents of neighboring molecules as described above, are clearly evidenced in Figure 12. Most likely based on vdW interactions, these conformational changes propagate within the monolayer from one molecule to its neighbors. Apart the instance of (C_{60}-**1**) → Ag(111) assembly, in which the fullerenes are presumably located on top of the macrocyclic core rings, any strong fullerene–porphyrin interactions are absent, as the C_{60} molecules are located between the porphyrin modules.

Therefore, we hypothesize that the observed long-range order of the hosted fullerene units in all-regular (C_{60}-p**1**) → Ag(111), (C_{60}-**1**) → Ag(111), and (C_{60}-**2**) → Ag(100) assemblies is most likely driven by the combination of two different interacting mechanisms: i) porphyrin-mediated coupling via local modifications of the hosting layer by the fullerene guest, i.e., through conformational or electronic adaptation; and ii) electronic interaction via the metal substrate.

Mechanism 1 contributes favorably to a regular fullerene arrangement via conformation-mediated intermolecular coupling. Upon deposition of a fullerene molecule onto any preformed porphyrin monolayer, both the electronic and the conformational structure of the single porphyrins surrounding a fullerene guest are expected to be affected, producing a change in their molecular conformation. Such molecular fluctuations may be tentatively attributed to the torsional flexure of the 3,5-di(*tert*-butyl)phenyl moieties, which are expected to be severely affected upon C_{60} deposition and were also observed after repositioning experiments on the adsorbed C_{60}. Such conformational changes are propagated over long distances through the compact porphyrin layer via attractive vdW and repulsive steric interactions. The contributions from mechanism 2 need to be considered as well, as the adsorption of a C_{60} molecule between porphyrin macrocycles is most likely accompanied by a charge-transfer process from the metal substrate to the C_{60} molecules. According to the models presented in Figures 4c and 10, the hosted C_{60} molecules are presumably not in direct contact with the metal substrate but rather lying on top of the 3-cyanophenyl substituents. For a monolayer of C_{60} in direct contact with Ag(111), a charge transfer of ca. 0.75 electrons per molecule has been experimentally measured.[66] Nevertheless, even at large distances (0.3 nm) from the metal surface, density functional studies predict a significant charge transfer of ca. 0.2 electrons per fullerene.[67] Such donation/back-donation of charges between the silver substrates and the hosted fullerene species could severely affect the surface electronic states, leading to surface-confined standing electron waves that might give rise to long-range interfullerene coupling, as observed for other molecular modules deposited on metal(111) surfaces.[68] Hence, these surface-confined waves

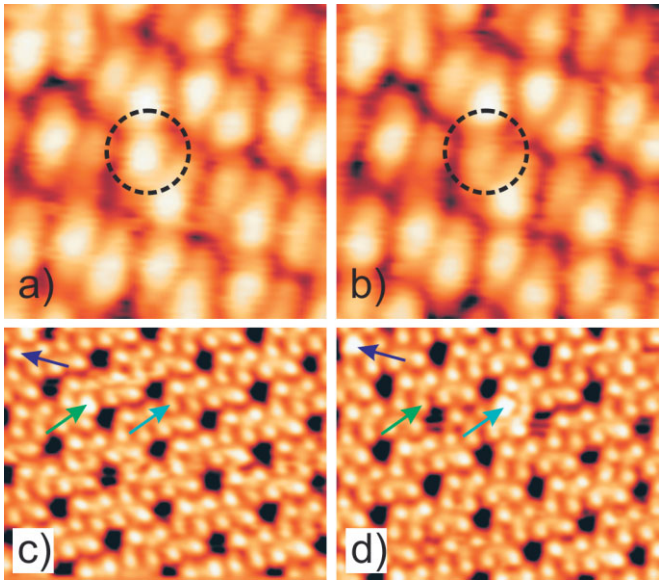

Figure 12. a,b) Time evolution of the conformations adopted by the 3,5-di(*tert*-butyl)phenyl substituents in a full monolayer of triply linked diporphyrin **2** (scan range: 7.8 nm × 7.6 nm, V_{bias} = 2.59 V, I_t = 11 pA, T = 298 K, the time lapse between (a) and (b) is 92 s). c,d) Porphyrin monomer **1** in the porous phase (scan range: 17.5 nm × 13.6 nm, V_{bias} = 2.86 V, I_t = 17 pA, T = 298 K, the time lapse between (c) and (d) is 62 s). The changes in apparent heights (circle and arrows) reflect the rotation of the 3,5-di(*tert*-butyl)phenyl substituents around the connecting σ-bond to the porphyrin core.

could ultimately contribute to the selective formation of the C_{60} chains, as observed in the (C_{60}-p**1**) → Ag(111) assembly.

5. Conclusions and Future Directions

In this article, we have summarized our investigations into the "bottom-up" fabrication of addressable multicomponent molecular entities obtained by self-assembly of C_{60} and porphyrins **1**–**4** on Ag(100) and Ag(111) surfaces (the synthesis of porphyrins **3** and **4** has been published elsewhere[69,70]). The first STM studies on ad-layers constituted of monomeric and triply linked porphyrin modules showed that the molecules self-organize into ordered assemblies, the structures of which are controlled by the porphyrin chemical structure, the substrate, and the surface coverage. Specifically, the first successful engineering of 2D porphyrin-based assemblies featuring regular structures with periodicities ranging from 2.2 to 7.5 nm on Ag surfaces has been reported. Subsequent co-deposition of C_{60} molecules on all porphyrin assemblies resulted in selective self-organization into ordered molecular-hybrid bilayers, the organization of which is driven by both fullerene coverage and porphyrin structure. Sublimation of C_{60} on top of a porous porphyrin network revealed the selective inclusion of the fullerene guests within the hosting cavities arranged in a nanopatterned array. In all-ordered fullerene–porphyrin assemblies, the C_{60} guests organize in unusual long chains and/or 2D arrays. The observed mode of fullerene self-assembly originates from a delicate equilibrium between substrate–molecule and molecule–molecule interactions involving charge-transfer processes and conformational flexibility that is a consequence of the structural adaptation of the fullerene–porphyrin bilayer. The work described here provides an intriguing example of a multicomponent supramolecular approach as a valid alternative for the fabrication of addressable molecular architectures. The possibility to produce large periodicities of up to 7.5 nm out of 2 nm building blocks may additionally contribute to overcoming the technological gap between "top-down" and "bottom-up" approaches in surface-structuring processes.

However, molecular assemblies obtained on solid substrates, formed by molecular entities that interact via a sum of unspecific weak interactions such as dipolar and van der Waals forces (i.e., like those reported in this work), hardly show any potential for applications in real devices because of the lack of stability and structural reversibility when under working conditions, such as in the presence of any external manipulating events, i.e., light or electrochemical induction. Therefore, our perspectives for future work are focused on overcoming such drawbacks by utilizing strong, directional intermolecular interactions, which are envisaged as being able to diminish the effect of a number of weaker interactions, thus achieving a much greater capacity for engineering and design of supramolecular assemblies. Specifically, the synthetic versatility of porphyrin modules should allow the implementation of further functionalities, which would enable adaptation of the physicochemical properties of the nanostructured surfaces to specific structural and applicative demands. Amongst the classical intermolecular interactions for the formation of supramolecular species, which can be compatible with real applications, we intend to use multiple hydrogen bonding.[15–17] Hence, we envisage being able to exploit multiple-hydrogen-bonding arrays for the formation of exceptionally robust organic networks featuring pre-organized domains, i.e., pores, showing hosting properties towards functional molecules such as fullerenes and other interesting π-systems.

Received: July 2, 2006
Revised: November 15, 2006
Published online: April 3, 2007

[1] R. Garcia, R. V. Martinez, J. Martinez, *Chem. Soc. Rev.* **2006**, *35*, 29.
[2] A. Credi, *Aust. J. Chem.* **2006**, *59*, 157.
[3] N. Nishiyama, K. Kataoka, *Nippon Rinsho* **2006**, *64*, 199.
[4] A. C. Grimsdale, K. Müllen, *Angew. Chem.* **2005**, *117*, 5732; *Angew. Chem. Int. Ed.* **2005**, *44*, 5592.
[5] J. P. Spatz, *Angew. Chem.* **2002**, *114*, 3507; *Angew. Chem. Int. Ed.* **2002**, *41*, 3359.
[6] A. Zangwill, *Physics at Surfaces*, Cambridge University Press, Cambridge, UK **1988**.
[7] J.-M. Lehn, *Science* **2002**, *295*, 2400.
[8] J.-M. Lehn, *Supramolecular Chemistry: Concepts and Perspectives*, Wiley-VCH, Weinheim, Germany **1998**.
[9] D. N. Reinhoudt, M. Crego-Calama, *Science* **2002**, *295*, 2403.
[10] G. M. Whitesides, B. Grzybowski, *Science* **2002**, *295*, 2418.
[11] T. Kato, *Science* **2002**, *295*, 2414.
[12] O. Ikkala, G. ten Brinke, *Science* **2002**, *295*, 2407.
[13] M. D. Hollingsworth, *Science* **2002**, *295*, 2410.
[14] a) A. M. Garcia, F. J. Romero-Salguero, D. M. Bassani, J.-M. Lehn, G. Baum, D. Fenske, *Chem. Eur. J.* **1999**, *5*, 1803. b) P. N. W. Baxter, J.-M. Lehn, B. O. Kneisel, D. Fenske, *Chem. Commun.* **1997**, 2231. c) P. N. W. Baxter, J.-M. Lehn, B. O. Kneisel, D. Fenske, *Angew. Chem.* **1997**, *109*, 1350; *Angew. Chem. Int. Ed. Engl.* **1997**, *36*, 1978. d) G. S. Hanan, D. Volkmer, U. S. Schubert, J.-M. Lehn, G. Baum, D. Fenske, *Angew. Chem.* **1997**, *109*, 1929; *Angew. Chem. Int. Ed. Engl.* **1997**, *36*, 1842.
[15] a) K. G. Nath, O. Ivasenko, J. A. Miwa, H. Dang, J. D. Wuest, A. Nanci, D. F. Perepichka, F. Rosei, *J. Am. Chem. Soc.* **2006**, *128*, 4212. b) S. De Feyter, A. Miura, S. Yao, Z. Chen, F. Wurthner, P. Jonkheijm, A. Schenning, E. W. Meijer, F. C. De Schryver, *Nano Lett.* **2005**, *5*, 77. c) F. C. De Schryver, S. De Feyter, *Chem. Soc. Rev.* **2003**, *32*, 139. d) S. De Feyter, F. C. De Schryver, *J. Phys. Chem. B* **2005**, *109*, 4290. e) S. Furukawa, H. Uji-i, K. Tahara, T. Ichikawa, M. Sonoda, F. C. De Schryver, Y. Tobe, S. De Feyter, *J. Am. Chem. Soc.* **2006**, *128*, 3502.
[16] a) M. Stöhr, M. Wahl, C. H. Galka, T. Riehm, T. A. Jung, L. H. Gade, *Angew. Chem.* **2005**, *117*, 7560; *Angew. Chem. Int. Ed.* **2005**, *44*, 1. b) L. M. A. Perdigao, N. R. Champness, P. H. Beton, *Chem. Commun.* **2006**, 538.
[17] a) P. Samorí, V. Francke, K. Müllen, J. P. Rabe, *Chem. Eur. J.* **1999**, *5*, 2312. b) K. Eichhorst-Gerner, A. Stabel, G. Moessner, D. Declerq, S. Valiyaveettil, V. Enkelmann, K. Müllen, J. P. Rabe, *Angew. Chem.* **1996**, *108*, 1599; *Angew. Chem. Int. Ed. Engl.* **1996**, *35*, 1492. c) G. Gottarelli, S. Masiero, E. Mezzina, S. Pieraccini, J. P. Rabe, P. Samorí, G. P. Spada, *Chem. Eur. J.* **2000**, *6*, 3242.
[18] T. Yokoyama, S. Yokoyama, T. Kamikado, Y. Okuno, S. Mashiko, *Nature* **2001**, *413*, 619.
[19] P. A. Liddell, J. P. Sumida, A. N. Macpherson, L. Noss, G. R. Seely, K. N. Clark, A. L. Moore, T. A. Moore, D. Gust, *Photochem. Photobiol.* **1994**, *60*, 537.
[20] a) H. Uji-i, A. Miura, A. Schenning, E. W. Meijer, Z. J. Chen, F. Wurthner, F. C. De Schryver, M. Van der Auweraer, S. De Feyter, *ChemPhysChem* **2005**, *6*, 2389. b) E. Mena-Osteritz, P. Bauerle, *Adv. Mater.* **2006**, *18*, 447.

[21] a) F. Langa, M. J. Gomez-Escalonilla, J.-M. Rueff, T. M. Figueira Duarte, J.-F. Nierengarten, V. Palermo, P. Samorì, Y. Rio, G. Accorsi, N. Armaroli, *Chem. Eur. J.* **2005**, *11*, 4405. b) J. A. Theobald, N. S. Oxtoby, M. A. Phillips, N. R. Champness, P. H. Beton, *Nature* **2003**, *424*, 1029.
[22] P. Samorì, A. Fechtenkötter, E. Reuther, M. D. Watson, N. Severin, K. Müllen, J. P. Rabe, *Adv. Mater.* **2006**, *18*, 1317.
[23] P. Samorí, H. Engelkamp, P. de Witte, A. E. Rowan, R. J. M. Nolte, J. P. Rabe, *Angew. Chem.* **2001**, *113*, 2410; *Angew. Chem. Int. Ed.* **2001**, *40*, 2348.
[24] L. Pirondini, A. G. Stendardo, S. Geremia, M. Campagnolo, P. Samori, J. P. Rabe, R. Fokkens, E. Dalcanale, *Angew. Chem.* **2003**, *115*, 1422; *Angew. Chem. Int. Ed.* **2003**, *42*, 1384.
[25] D. G. Kurth, N. Severin, J. P. Rabe, *Angew. Chem. Int. Ed.* **2002**, *41*, 3681.
[26] a) N. Lin, S. Stepanow, F. Vidal, J. V. Barth, K. Kern, *Chem. Commun.* **2005**, 1681. b) A. Dmitriev, H. Spillmann, N. Lin, J. V. Barth, K. Kern, *Angew. Chem.* **2003**, *115*, 2774; *Angew. Chem. Int. Ed.* **2003**, *42*, 2670. c) A. Semenov, J. P. Spatz, M. Moller, J.-M. Lehn, B. Sell, D. Schubert, C. H. Weidl, U. S. Schubert, *Angew. Chem.* **1999**, *111*, 2701; *Angew. Chem. Int. Ed.* **1999**, *38*, 2547. d) M. S. Alam, S. Stromsdorfer, V. Dremov, P. Muller, J. Kortus, M. Ruben, J.-M. Lehn, *Angew. Chem.* **2005**, *117*, 8021; *Angew. Chem. Int. Ed.* **2005**, *44*, 7896. e) U. Ziener, J.-M. Lehn, A. Mourran, M. Moller, *Chem. Eur. J.* **2002**, *8*, 951.
[27] Y.-B. Wang, Z. Lin, *J. Am. Chem. Soc.* **2003**, *125*, 6072.
[28] F. Wudl, *Acc. Chem. Res.* **1992**, *25*, 157.
[29] L. Echegoyen, L. E. Echegoyen, *Acc. Chem. Res.* **1998**, *31*, 593.
[30] L. R. Milgron, *The Colours of Life: An Introduction to the Chemistry of Porphyrins and Related Compounds*, Oxford University Press, Oxford, UK **1997**.
[31] D. M. Guldi, M. Prato, *Acc. Chem. Res.* **2000**, *33*, 695.
[32] D. M. Guldi, *Chem. Commun.* **2000**, 321.
[33] D. Bonifazi, G. Accorsi, N. Armaroli, F. Song, A. Palkar, L. Echegoyen, M. Scholl, P. Seiler, B. Jaun, F. Diederich, *Helv. Chim. Acta* **2005**, *88*, 1839.
[34] P. D. W. Boyd, C. A. Reed, *Acc. Chem. Res.* **2005**, *38*, 235.
[35] M. R. Wasielewski, *Chem. Rev.* **1992**, *92*, 435.
[36] D. Gust, T. A. Moore, A. L. Moore, *Acc. Chem. Res.* **2001**, *34*, 40.
[37] D. M. Guldi, S. Fukuzumi, *J. Porphyr. Phthalocyanines* **2002**, *6*, 289.
[38] H. Imahori, Y. Mori, Y. Matano, *J. Photochem. Photobiol. C* **2003**, *4*, 51.
[39] H. Imahori, Y. Sakata, *Eur. J. Org. Chem.* **1999**, 2445.
[40] N. Armaroli, *Photochem. Photobiol. Sci.* **2003**, *2*, 73.
[41] N. Armaroli, G. Marconi, L. Echegoyen, J. P. Bourgeois, F. Diederich, *Chem. Eur. J.* **2000**, *6*, 1629.
[42] a) W.-D. Schneider, *Phys. Status Solidi A* **2001**, *187*, 125. b) S. De Feyter, A. Gesquiere, M. M. Abdel-Mottaleb, P. C. M. Grim, F. C. De Schryver, C. Meiners, M. Sieffert, S. Valiyaveettil, K. Mullen, *Acc. Chem. Res.* **2000**, *33*, 520.
[43] J. Otsuki, E. Nagamine, T. Kondo, K. Iwasaki, M. Asakawa, K. Miyake, *J. Am. Chem. Soc.* **2005**, *127*, 10 400.
[44] a) S. Yoshimoto, N. Yokoo, T. Fukuda, N. Kobayashi, K. Itaya, *Chem. Commun.* **2006**, 500. b) S. Yoshimoto, S. Sugawara, K. Itaya, *Electrochemistry* **2006**, *74*, 175.
[45] H. Ma, L.-Y. O. Yang, N. Pan, S.-L. Yau, J. Jiang, K. Itaya, *Langmuir* **2006**, *22*, 2105.
[46] J. A. A. W. Elemans, R. van Hameren, R. J. M. Nolte, A. E. Rowan, *Adv. Mater.* **2006**, *18*, 1251.
[47] S. Yoshimoto, N. Higa, K. Itaya, *J. Am. Chem. Soc.* **2004**, *126*, 8540.
[48] S. Yoshimoto, Y. Honda, Y. Murata, M. Murata, K. Komatsu, O. Ito, K. Itaya, *J. Phys. Chem. B* **2005**, *109*, 8547.
[49] D. Bonifazi, H. Spillmann, A. Kiebele, M. de Wild, P. Seiler, F. Cheng, H.-J. Güntherodt, T. Jung, F. Diederich, *Angew. Chem.* **2004**, *116*, 4863; *Angew. Chem. Int. Ed.* **2004**, *43*, 4759.
[50] H. Spillmann, A. Kiebele, M. Stöhr, T. A. Jung, D. Bonifazi, F. Cheng, F. Diederich, *Adv. Mater.* **2006**, *18*, 275.
[51] S. Yoshimoto, E. Tsutsumi, Y. Honda, Y. Murata, M. Murata, K. Komatsu, O. Ito, K. Itaya, *Angew. Chem.* **2004**, *116*, 3106; *Angew. Chem. Int. Ed.* **2004**, *43*, 3044.
[52] T. Jung, R. R. Schlitter, J. K. Gimzewski, H. Tang, C. Joachim, *Science* **1996**, *271*, 181.
[53] T. Jung, R. R. Schlitter, J. K. Gimzewski, *Nature* **1997**, *386*, 696.
[54] D. Bonifazi, M. Scholl, F. Y. Song, L. Echegoyen, G. Accorsi, N. Armaroli, F. Diederich, *Angew. Chem.* **2003**, *115*, 5116; *Angew. Chem. Int. Ed.* **2003**, *42*, 4966.
[55] All STM images were recorded with high tunnelling-gap resistance (> 100 GΩ) to reduce the influence of the tip on the hopping processes.
[56] A. Kiebele, D. Bonifazi, F. Cheng, M. Stöhr, F. Diederich, T. Jung, H. Spillmann, *ChemPhysChem* **2006**, *7*, 1462.
[57] A. Tsuda, H. Furuta, A. Osuka, *Angew. Chem.* **2000**, *112*, 2649; *Angew. Chem. Int. Ed.* **2000**, *39*, 2549.
[58] A. Tsuda, F. Furuta, A. Osuka, *J. Am. Chem. Soc.* **2001**, *123*, 10 304.
[59] J. Kuntze, X. Ge, R. Berndt, *Nanotechnology* **2002**, *13*, S337.
[60] F. Moresco, G. Meyer, K.-H. Rieder, H. Tang, A. Gourdon, C. Joachim, *Phys. Rev. Lett.* **2001**, *86*, 672.
[61] F. Moresco, G. Meyer, K.-H. Rieder, J. Ping, H. Tang, C. Joachim, *Surf. Sci.* **2002**, *499*, 94.
[62] For a recent comprehensive review on multipolar interactions, including those between cyano dipoles, see: R. Paulini, K. Müller, F. Diederich, *Angew. Chem.* **2005**, *117*, 1820; *Angew. Chem. Int. Ed.* **2005**, *44*, 1788.
[63] M. de Wild, S. Berner, H. Suzuki, H. Yanagi, D. Schlettwein, S. Ivan, A. Baratoff, H.-J. Güntherodt, T. A. Jung, *ChemPhysChem* **2002**, *3*, 881.
[64] M. Böhringer, W.-D. Schneider, R. Berndt, *Surf. Sci.* **1998**, *408*, 72.
[65] C. Pan, M. P. Sampson, Y. Chai, R. H. Hauge, J. L. Margrave, *J. Phys. Chem.* **1991**, *95*, 2944.
[66] E. I. Altman, R. J. Colton, *Phys. Rev. B* **1993**, *48*, 18 244.
[67] L.-L. Wang, H.-P. Cheng, *Phys. Rev. B* **2004**, *69*, 165 417.
[68] a) J. Repp, F. Moresco, G. Meyer, K.-H. Rieder, *Phys. Rev. Lett.* **2000**, *85*, 2981. b) S. Lukas, G. Witte, C. Wöll, *Phys. Rev. Lett.* **2002**, *88*, 028 301. c) V. S. Stepanyuk, A. N. Baranov, D. V. Tsivlin, W. Hergert, P. Bruno, N. Knorr, M. A. Schneider, K. Kern, *Phys. Rev. B* **2003**, *68*, 205, 410.
[69] F. Cheng, S. Zhang, A. Adronov, L. Echegoyen, F. Diederich, *Chem. Eur. J.* **2006**, *12*, 6062.
[70] M. Kamo, A. Tsuda, Y. Nakamura, N. Aratani, K. Furukawa, T. Kato, A. Osuka, *Org. Lett.* **2003**, *5*, 2079.